

Azimuthal decomposition study of a realistic laser profile for efficient modeling of Laser WakeField Acceleration

I. Zemzemi¹, F. Massimo¹, A. Beck¹

¹ Laboratoire Leprince-Ringuet – École polytechnique, CNRS-IN2P3, Palaiseau 91128, France

E-mail: izemzemi@l1r.in2p3.fr

Abstract. The advent of ultra short high intensity lasers has paved the way to new and promising, yet challenging, areas of research in the laser-plasma interaction physics. The success of constructing petawatt femtosecond lasers, for instance the Apollon laser in France, will help understanding and designing future particle accelerators and next generation of light sources. Achieving this goal intrinsically relies on the combination between experiments and massively parallel simulations. So far, Particle-In-Cell (PIC) codes have been the ultimate tool to accurately describe the laser-plasma interaction especially in the field of Laser WakeField Acceleration (LWFA). Nevertheless, the numerical modelling of laser plasma accelerators in 3D can be a very challenging task. This is due to the large dispersity between the scales involved in this process. In order to make such simulations feasible with a significant speed up, we need to use reduced numerical models which simplify the problem while retaining a high fidelity. Among these models, Fourier field decomposition in azimuthal modes for the cylindrical geometry [1] is a promising reduced model especially for physical problems that have close to cylindrical symmetry which is the case in LWFA. This geometry has been implemented in the open-source code SMILEI [2] in Finite Difference Time Domain (FDTD) discretization scheme for the Maxwell solver. In this paper we will study the case of a realistic laser measurement from Apollon facility, the ability of this method to describe it correctly and the determination of the necessary number of modes for this purpose. We will also show the importance of higher modes inclusion in the case of realistic laser profiles to insure fidelity in simulation.

1. Introduction

The continuous upgrade in laser power has permitted the investigation and the verification of new methods of particle acceleration by taking advantage from the high gradient wakefield created when the laser propagates through an under-dense plasma. Laser WakeField Acceleration (LWFA) [3] [4] [5] has been proven to be a promising efficient way to accelerate electrons up to few GeVs within a short propagation of distance with high quality of beam. In order to investigate the different experimental set-ups and to determine the optimal parameters to achieve this goal, simulation is the key to perform a parametric scan and analyze regimes that haven't been explored yet. That one may model correctly the interaction between the laser and the plasma, a full kinetic description of the plasma is needed. Particle-in-Cell code is ubiquitously used as an established tool that solves Vlasov equation for the different species presented in the plasma coupled with Maxwell equations. It is a powerful method that gives an accurate description of the plasma response to the laser and captures a wide range of physical phenomena [6]. Nevertheless,

precise and realistic results are obtained only with full 3D description with high resolution. Even though 2D simulations are used in the context of 2D Cartesian slab or in the cylindrical geometry r-z to illuminate the physics, there is a qualitative and quantitative difference with the 3D simulation especially in the case of LWFA when studying non linear regime. This is mainly because self focus and self modulation of the phase are not well described by a 2D simulation [7]. In spite of the necessity of using well resolved 3D simulation for the accurate description, using many points in the grid for long propagation distance with small time steps is very costly and pushes the existent computing resources available nowadays to the limits in order to have the simulation results in a reasonable amount of time. Therefore, there have been many methods suggested to overcome this obstacle among which we mention moving window, quasi-static approximation [8], ponderomotive guiding center or envelope description [9], boosted frame [10] ... Each method has its advantages and its limits depending on the case of study.

Thanks to the close to cylindrical symmetry of the laser in LWFA, an alternative has been proposed to reduce the cost of the simulations while retaining high fidelity [1]. In section 2, the main features of the algorithm are recalled and section 3 shows a study of the number of modes required to mimic the realistic Apollon laser profile correctly.

2. Review of the Azimuthal Fourier decomposition in cylindrical geometry

In this algorithm, the fields $\mathbf{E}, \mathbf{B}, \mathbf{J}, \rho$ in cylindrical coordinates (r, z, θ) are decomposed in Fourier space in θ direction according to (1) and (2).

$$F(r, z, \theta) = \sum_{m=-\infty}^{\infty} \tilde{F}_m(r, z) e^{-im\theta} \quad \text{with} \quad \tilde{F}_m(r, z) = \frac{1}{2\pi} \int_0^{2\pi} d\theta F(r, z, \theta) e^{im\theta} \quad (1)$$

$$\begin{aligned} F(r, z, \theta) &= \tilde{F}_0(r, z) + \sum_{m=1}^{\infty} \text{Re} \left[2\tilde{F}_m(r, z) e^{-im\theta} \right] \\ &= \tilde{F}_0(r, z) + \sum_{m=1}^{\infty} \text{Re} \left[2\tilde{F}_m(r, z) \right] \cos(m\theta) + \text{Im} \left[2\tilde{F}_m(r, z) \right] \sin(m\theta) \end{aligned} \quad (2)$$

This expansion is replaced in Maxwell equations and thanks to their linearity, it generates a set of equations (3).

$$\begin{aligned} \frac{\partial \tilde{B}_{r,m}}{\partial t} &= \frac{im}{r} \tilde{E}_{z,m} + \frac{\partial \tilde{E}_{\theta,m}}{\partial z} \\ \frac{\partial \tilde{B}_{\theta,m}}{\partial t} &= -\frac{\partial \tilde{E}_{r,m}}{\partial z} + \frac{\partial \tilde{E}_{z,m}}{\partial r} \\ \frac{\partial \tilde{B}_{z,m}}{\partial t} &= -\frac{1}{r} \frac{\partial(r \tilde{E}_{\theta,m})}{\partial r} - \frac{im}{r} \tilde{E}_{r,m} \\ \frac{1}{c^2} \frac{\partial \tilde{E}_{r,m}}{\partial t} &= -\frac{im}{r} \tilde{B}_{z,m} - \frac{\partial \tilde{B}_{\theta,m}}{\partial z} - \mu_0 \tilde{J}_{r,m} \\ \frac{1}{c^2} \frac{\partial \tilde{E}_{\theta,m}}{\partial t} &= \frac{\partial \tilde{B}_{r,m}}{\partial z} - \frac{\partial \tilde{B}_{z,m}}{\partial r} - \mu_0 \tilde{J}_{\theta,m} \\ \frac{1}{c^2} \frac{\partial \tilde{E}_{z,m}}{\partial t} &= \frac{1}{r} \frac{\partial(r \tilde{B}_{\theta,m})}{\partial r} + \frac{im}{r} \tilde{B}_{r,m} - \mu_0 \tilde{J}_{z,m} \end{aligned} \quad (3)$$

Each mode evolves independently in vacuum and different modes are coupled only when the plasma is present. The Fourier series in equations 1 and 2 is usually truncated up to very first modes in the case of low dependence on θ . For example, wakefields can be described by mode 0 because it is independent from θ and the laser by mode 1. In fact, for a cylindrically symmetric pulse (for example a gaussian one) propagating in z and polarized linearly along $\vec{e}_\alpha = \cos(\alpha)\vec{e}_x + \sin(\alpha)\vec{e}_y$, the field component \vec{E} depends on θ according to the following description:

$$\begin{aligned}
\vec{E} &= E_0(r, z)\vec{e}_\alpha \\
&= E_0(r, z)[\cos(\alpha)(\cos(\theta)\vec{e}_r - \sin(\theta)\vec{e}_\theta) + \sin(\alpha)(\sin(\theta)\vec{e}_r + \cos(\theta)\vec{e}_\theta)] \\
&= \text{Re}[E_0(r, z)e^{i\alpha}e^{-i\theta}]\vec{e}_r + \text{Re}[-iE_0(r, z)e^{i\alpha}e^{-i\theta}]\vec{e}_\theta \\
&= E_r\vec{e}_r + E_\theta\vec{e}_\theta
\end{aligned} \tag{4}$$

Here the amplitude E_0 does not depend on θ because the pulse was assumed to be cylindrically symmetric. In this case, the above relation shows that the fields E_r and E_θ of the laser are represented exclusively by the mode $m = 1$ and the same stands for B_r and B_θ . Thus, any cylindrically symmetric laser can be thoroughly described by the mode 1. As a consequence, the infinite sum of modes can be truncated at the first two modes since only the modes $m = 0$ and $m = 1$ are necessary to model laser-wakefield acceleration with linearly polarized lasers with axisymmetric envelope such as gaussian ones.

However, realistic lasers are not perfectly gaussian and because of their imperfections and spatio-temporal couplings [11] [12] they lose their symmetry and thus an accurate model of realistic laser profiles includes more than just two modes. This is why, m_{max} the maximal number of modes used is kept as a free parameter in the implementation of the method.

3. Experimental laser focal spot data analysis

In this section, the optimal number of modes to include in simulations is defined and the impact of the laser envelope imperfections on the decomposition is shown. For this purpose, the experimental intensity distribution in the focal plan from Apollon laser is used as input in this study. However, spatio-temporal distortions, i.e spatial dependencies of the temporal properties are not taken into consideration. A gaussian time envelope was assumed in this study. The figure 1 shows the measured intensity in the focal plan of the Apollon laser. Intensity is normalized to laser strength parameter a_0 . The raw data from the camera was interpolated to the simulation grid using a quadratic interpolation function taking into account the number of pixels of the camera and the pixel size. Table 1 sums up the laser parameters for this analysis.

Qualitatively, we can see from the reconstructed fields in figure 2 that the more modes we take into consideration, the closer we get to the real laser field and the more asymmetry appears in the reconstructed field. For example, the 2 modes (mode 0 + mode 1) reconstructed field has an envelope that is perfectly axis-symmetric and that the intensity distribution surrounding the main spot is homogeneous and symmetric. However, more contrast and heterogeneity appear in this area with higher number of modes.

Even though including higher modes in the reconstruction process is important to reproduce the heterogeneity in the intensity distribution, figure 3 shows that most of this intensity is represented exclusively by mode 1, which is the only non-zero mode in the case of cylindrically-symmetric laser, and other modes have lower contributions (note the different color bars for each panel). This is confirmed by the figure 4, that exhibits the distribution of the relative energy norm contained in each mode separately. The relative energy norm per mode was calculated as $\frac{\|E_{mode}\|_2}{\|E_{laser}\|_2}$ with the energy norm of a $2D$ discrete signal x calculated according

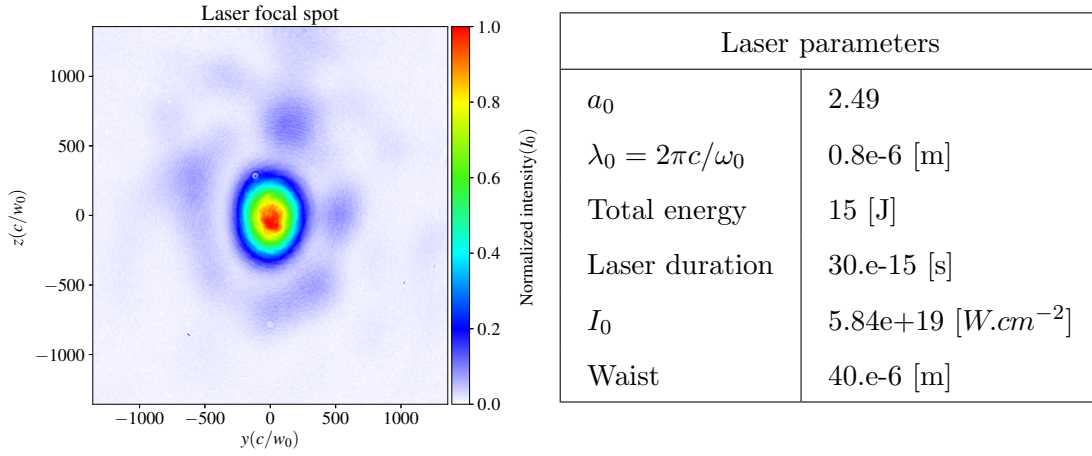


Figure 1: Laser intensity in the focal plan from experimental measurement.

Table 1: Laser parameters with λ_0 the laser wavelength and ω_0 its frequency.

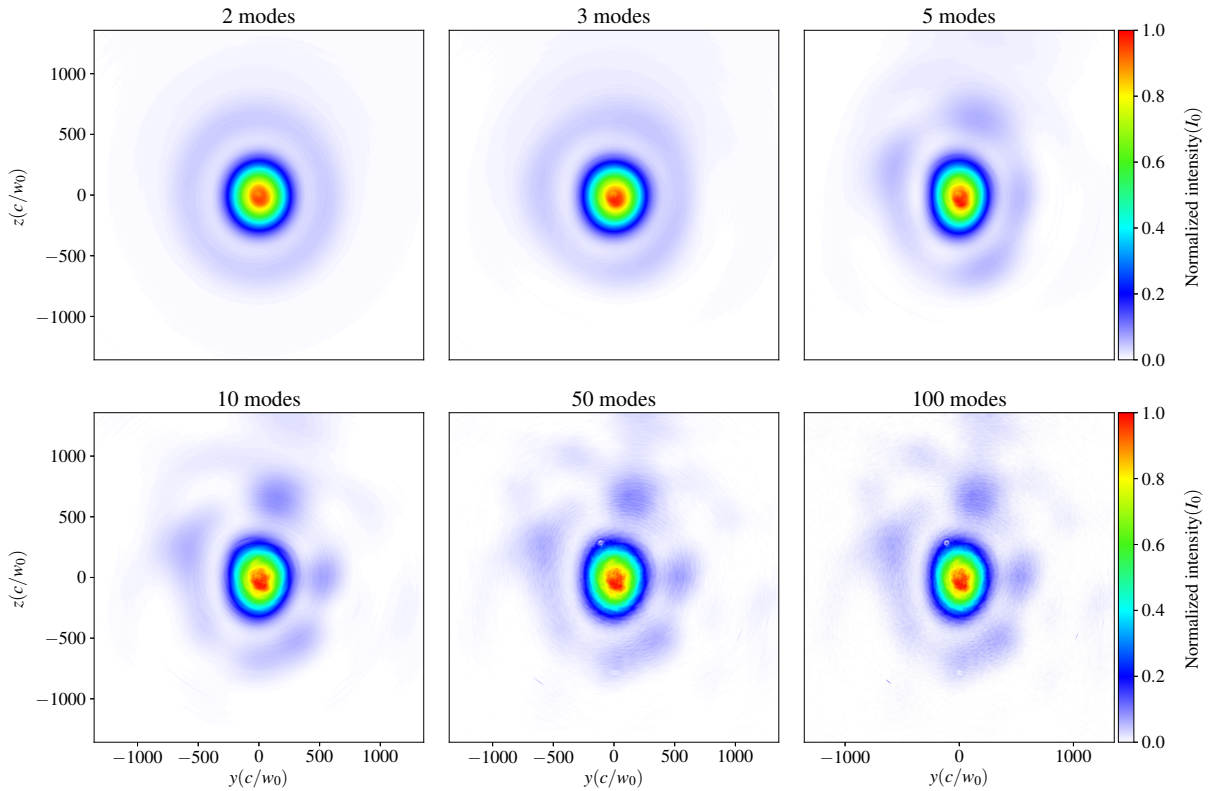


Figure 2: Normalized intensity of reconstructed laser field varying the number of modes .

to: $\|x\|_2 = \sum_{i,j} |x_{i,j}|^2$. The mode 1 has almost the entire energy of the laser and small portions are distributed unequally between the different modes: lower modes have more energy than the higher ones. Their contribution decreases with the number of modes.

Figure 5 shows the evolution of the relative energy norm error of the reconstructed field $\frac{\|E_{reconstructed}\|_2}{\|E_{laser}\|_2}$ in function of the number of modes used for the reconstruction with logarithmic scale along y axis. Left panel shows that the error decreases very quickly up to the first 20

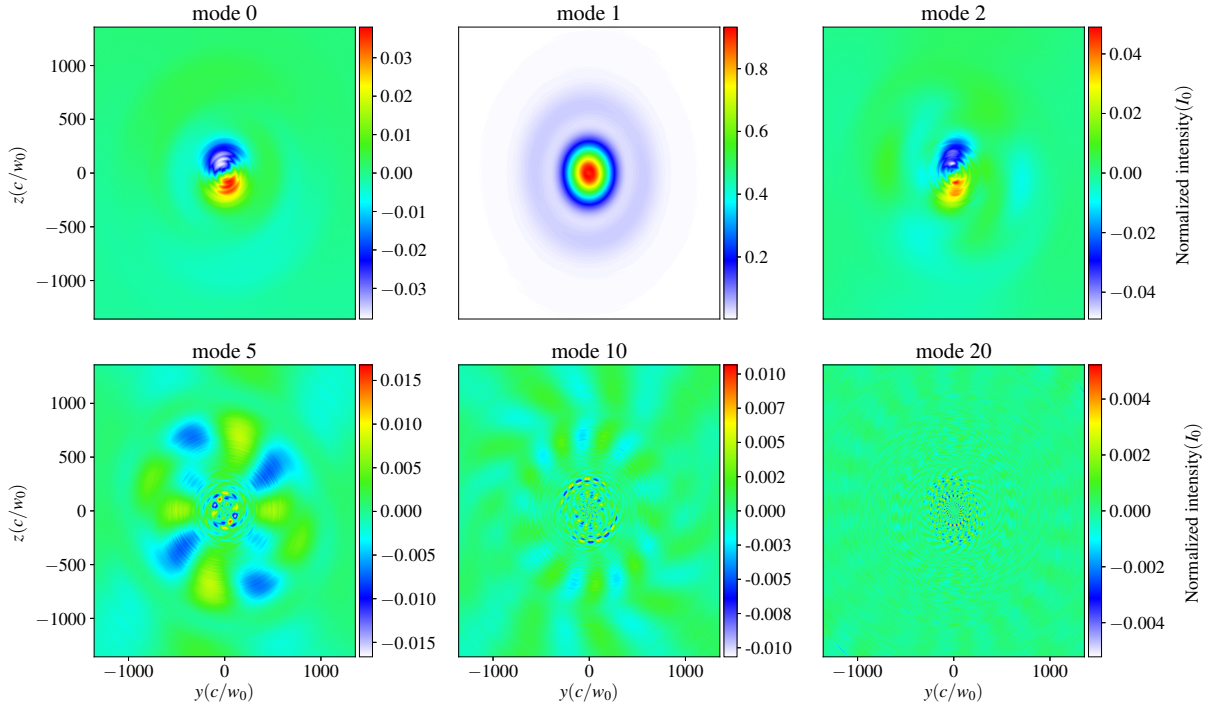


Figure 3: Normalized intensity of reconstructed laser fields in each mode separately.

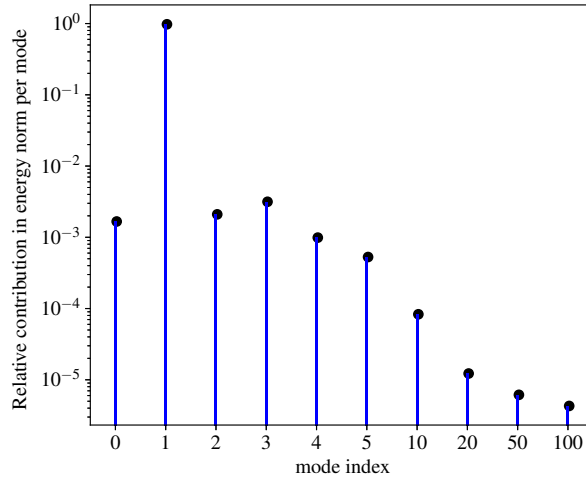


Figure 4: Relative energy norm of the reconstructed fields for a sample of modes

modes. This means that the optimal number of modes, which gives a good approximation of the real laser, is to be chosen between 2 and 20. The panel on the right is a close up of the panel on the left limiting the number of modes to the first 20 ones. Even though, we restrain m_{max} to 20, using 20 modes in the simulation is still very expensive for two reasons: First, the cost of the simulation with this geometry doesn't increase linearly with the number of modes because higher number of modes requires a higher number of particles per cell. Second, the Courant–Friedrichs–Lewy (CFL) condition of the azimuthal FDTD scheme depends on m_{max} , it becomes more strict with higher modes and implies smaller time step to avoid instabilities

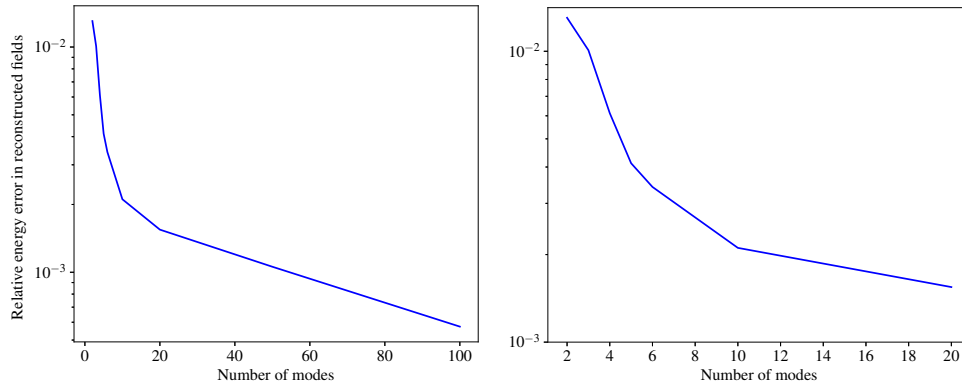


Figure 5: Relative energy error of the reconstructed fields: on the left number of modes up to 100, on the right a close up to modes up to 20.

induced by the discretization scheme. Therefore, from figures 2 and 5 it seems that 5 modes is a good compromise between precision and a reasonable simulation cost. This analysis is a crucial step to the plugging of realistic lasers profiles in simulations run with the azimuthal cylindrical geometry

4. Conclusion

We have reviewed briefly the basics of the azimuthal Fourier field decomposition and how it can achieve a gain in numerical simulation cost with it. We have also proved its ability to describe realistic laser even with a low number of modes. Hence, this method combines precision, fidelity and speed up. However, a more accurate study should be carried not only on the focal spot of the laser but also with a correct reconstructed phase from the different measurements around the focal plan which may increase the needed number of modes to describe the laser evolution correctly.

Acknowledgments

We are grateful to Julien Derouillat for his dedication to help implementing this algorithm in SMILEI in an efficient way, to Frederic Perez for his help with the development of the post processing tool Happi to include this geometry, to Arnd Specka for his role of medium with the experimentalists and for the fruitful discussions and to Dimitris Papadopoulos and his team for providing us with the data. Imen Zemzemi is thankful to Haithem Kallala for the discussions about Fourier transform and Python tools to reconstruct the fields. F. Massimo was supported by P2IO LabEx (ANR-10-LABX-0038) in the framework “Investissements d’Avenir” (ANR-11-IDEX-0003-01) managed by the Agence Nationale de la Recherche (ANR, France).

References

- [1] Lifschitz A, Davoine X, Lefebvre E, Faure J, Rechatin C and Malka V 2009 *Journal of Computational Physics* **228** 1803 – 1814 ISSN 0021-9991
- [2] Derouillat J, Beck A, Pérez F, Vinci T, Chiamello M, Grassi A, Flé M, Bouchard G, Plotnikov I, Aunai N, Dargent J, Riconda C and Grech M 2018 *Computer Physics Communications* **222** 351 – 373 ISSN 0010-4655
- [3] Tajima T and Dawson J M 1979 *Phys. Rev. Lett.* **43**(4) 267–270
- [4] Esarey E, Schroeder C B and Leemans W P 2009 *Rev. Mod. Phys.* **81**(3) 1229–1285
- [5] Malka V, Fritzier S, Lefebvre E, Aeonard M M, Burgy F, Chambaret J P, Chemin J F, Krushelnick K, Malka G, Mangles S P D, Najmudin Z, Pittman M, Rousseau J P, Scheurer J N, Walton B and Dangor A E 2002 *Science* **298** 1596–1600 ISSN 0036-8075

- [6] Birdsall C K and Langdon A B 2004 *Plasma Physics via Computer Simulation* (Taylor and Francis Group)
- [7] Davoine X, Lefebvre E, Faure J, Rechatin C, Lifschitz A and Malka V 2008 *Physics of Plasmas* **15** 113102
- [8] Mora P and Thomas M Antonsen J 1997 *Physics of Plasmas* **4** 217–229
- [9] Benedetti C, Schroeder C B, Esarey E, Geddes C G R and Leemans W P 2010 *AIP Conference Proceedings* **1299** 250–255
- [10] Vay J L 2007 *Phys. Rev. Lett.* **98**(13) 130405
- [11] Pariente G and Quéré F 2015 *Opt. Lett.* **40** 2037–2040 URL <http://ol.osa.org/abstract.cfm?URI=ol-40-9-2037>
- [12] Jeandet A, Borot A, Nakamura K, Leemans W, Pariente G, Sainte-Marie A, Gobert O and Quéré F 2018 Spatio-temporal couplings of ultrashort lasers: Metrology and applications *High-Brightness Sources and Light-driven Interactions* (Optical Society of America) p HW3D.1